Orthogonal Frequency Division Multiplexing With Joint Subblocks Index Modulation

YUXIN SHI[ID], KAI GAO, JIANG ZHU[ID], XINJIN LU[ID], AND SHILIAN WANG

College of Electronic Science, National University of Defense Technology, Changsha 410073, China

Corresponding author: Kai Gao (gaokai000@hotmail.com)

ABSTRACT Recently, orthogonal frequency division multiplexing (OFDM) with index modulation has emerged as promising technologies with the improvement of spectral efficiency and energy efficiency, which carries additional index bits through the index domain. In OFDM-IM, some indices of subcarrier activation patterns are discarded to retain a part of indices to convey index bits, which causes the loss of spectral efficiency. In this paper, we proposed a novel technique to combine indices of a part of subblocks, called OFDM with joint subblocks index modulation (OFDM-JS-IM), which is capable of enhancing the spectral efficiency and energy efficiency without extra energy consumption compared to OFDM-IM. The length of joint subblocks is also discussed to properly enhance spectral efficiency. Moreover, near the maximum-likelihood detector and low-complexity log-likelihood ratio detector are proposed to mitigate the high burden caused by joint subblocks. Theoretical analysis based on pairwise error probability is conducted which fits well with the simulation results. The Monte Carlo simulations show that the proposed scheme achieves improvement of spectral efficiency with slight performance loss in comparison with OFDM-IM.

INDEX TERMS OFDM-with index modulation (OFDM-IM), joint subblocks, spectral efficiency, subcarrier activation patterns, log-likelihood ratio detection.

I. INTRODUCTION

Orthogonal-frequency division multiplexing (OFDM) is a popular method for high rate transmission in wireless communications with its distinctive advantages. The main advantage of OFDM is its ability to cope with severe channel conditions such as narrowband interference and frequency-selective fading with simple equalization filters [1]. In the standard of long-term evolution (LTE), OFDM is the core of the downlink radio transmission [2], [3]. OFDM can also be combined with antenna arrays at the transmitter and receiver to increase the diversity gain or to enhance the system capacity on time-varying and frequency-selective channels, resulting in a multiple-input multiple-output (MIMO) configuration [4].

In recent years, Index modulation (IM) is an emerging energy saving concept firstly used in spatial modulation (SM) that carries additional information through the antenna indices [5]. Then the concept has been successfully transplanted to orthogonal frequency division multiplexing (OFDM) with index modulation, where the antenna indices are replaced by the indices of subcarriers.

The associate editor coordinating the review of this manuscript and approving it for publication was Maurizio Magarini.

Owing to the advantages of energy efficiency (EE) and spectral efficiency (SE), IM technique has been emerged as potential technique in 5G [6]–[8]. In [9], the subcarrier-index modulated OFDM (SIM-OFDM) was proposed to modulate a subset of subcarrirers according to an on-off keying data stream, but this scheme suffers from the underlying error propagation problem and unstable data rate. To address these issues, an enhanced SIM-OFDM scheme (ESIM-OFDM) was proposed by dividing subcarriers into pairs [10]. In each pair of subcarriers, only one subcarrier was activated, whose index carried one index binary bit. However, the SE of ESIM-OFDM scheme is lower than that of classical OFDM due to the small and fixed index structure. Hence, the way of fully utilization of subcarrier indices becomes an important issue of the index modulation schemes. In 2012, OFDM with index modulation (OFDM-IM) was put forward where the size of the subblock is more flexible by using two different mapping techniques called look-up table and combinatorial method to transmit information bits into index domain of the OFDM subblock [11]. However, the spectral efficiency of OFDM-IM is limited due to idle subcarriers of OFDM-IM. In [12], GIM-OFDM1 and GIM-OFDM2 were proposed to permit more legitimate indices by introducing various numbers of active subcarriers in each subblock and

two dimensions of index modulation in both in-phase and quadrature (I/Q) components respectively, which enhances the SE by transmitting more index bits. In [13], dual mode index modulation (DM-OFDM) was proposed, where the idle subcarriers were displaced by the other distinguishable constellation alphabets, which increases the SE by conveying more symbol bits. After that, [12] and [13] were combined by [14], called the generalized DM-OFDM and high SE is attained in this scheme. However, the better performance gained by OFDM-IM derived from its high diversity order of index bits, which means that more index bits are expected to improve the performance of system. In [15], zero is regarded as the third mode based on DM-OFDM scheme, which introduces extra indices that can be used to transmit index bits. In 2017, multiple-mode OFDM-IM (MM-OFDM-IM) [16] has been proposed to transmit information by multiple distinguishable modes and their full permutations, which achieves better performance by higher diversity order of index bits. Moreover, linear constellation precoding technique was used to harvest additional diversity gain in [17]. Recently, an adaptive subcarrier index aided with Huffman entropy coding principle was proposed, which can adaptively choose the probability used in Huffman coding to optimize either the channel capacity, or the error performance, or alternatively the EE of the system [18]. In [19], OFDM-IM with the codebook design can potentially provide a tradeoff between diversity and transmission rate. Applying the OFDM-IM to the network, an adaptive OFDM-IM for two-hop relay networks was proposed in [20]. Moreover, coordinate interleaving [21] and linear precoding [17] have been combined in [22], which aims to attain both the high diversity order and high spectral efficiency. However, the indices which can be converted into index bits may not be fully used due to the mismatch of the number of indices and binary index bits in most of index modulation schemes. As a result, some of indices are discarded in each subblock, which actually wastes a large number of indices. Therefore, the reuse of discarded indices is a significant way to increase the energy efficiency and spectral efficiency by transmitting extra index bits.

In this paper, OFDM with joint subblocks index modulation (OFDM-JS-IM) scheme is proposed where a subset of adjacent subblocks are combined to produce joint indices mapping to incoming index bits. With such arrangement, most indices which are discarded in OFDM-IM can be fully reused. Besides, a novel algorithm is put forward to transforming some single subblock indices into joint subblocks indices, which makes the index mapping operation simply. In the receiver, we discuss near maximum-likelihood (ML) detector and log-likelihood radio (LLR) detector for demodulation, which decreases the computational complex of the proposed scheme.

The rest of this paper is organized as follows. Section II describes the system model of OFDM-IM. In Section III, the principles of OFDM-JS-IM scheme which contain the transmitter model and the way of selecting the proper length of joint subblocks are illustrated. Afterward, Section IV

presents the two low-complexity detectors used in OFDM-JS-IM. Then analysis of OFDM-JS-IM BER performance based on pairwise error probability (PEP) approximation is conducted in Section V. The BER performance evaluations are presented in Section VI. Finally, the results are concluded in Section VII.

Notation: $\mathcal{X} \sim \mathcal{CN}(0, \sigma^2)$ represents the distribution of a circularly symmetrical complex Gaussian random variable $\mathcal{X}$ with the variance σ^2. $\lfloor \cdot \rfloor$ and $\lceil \cdot \rceil$ are the floor and ceiling operation respectively. I_N denotes the $N \times N$ dimension identity matrix. $C(\cdot, \cdot)$ denotes the binomial coefficient. $(\cdot)^T$ and $(\cdot)^H$ denote Hermitian transpose and transpose. $Q(\cdot)$ denotes the tail probability of the standard Gaussian distribution. $rank(X)$ returns the rank of a matrix X. $diag(x)$ creates a diagonal matrix whose diagonal elements are x. $\|\cdot\|_2$ denotes 2-norm of a matrix.

II. SYSTEM MODEL OF OFDM-IM

At the transmitter of OFDM-IM, N subcarriers are partitioned into g groups and each group has a subblock with n subcarriers. Considering the qth subblock, the OFDM-IM symbols modulated by subcarriers can be presented by

$$x^{(q)} = [x_{(q-1)n+1} \ x_{(q-1)n+2} , \ldots , x_{qn}]^T \quad 1 \leqslant q \leqslant g, \quad (1)$$

where each element of column vector x is 0 (idle subcarrier) or M-ary constellation signal (active subcarrier). In each subblock, the number of active subcarriers, k are fixed and therefore the number of subcarrier activation patterns (SAPs) are $C(n, k)$. Thus $\lfloor \log_2 C(n, k) \rfloor$ bits can be conveyed by $2^{\lfloor \log_2 C(n,k) \rfloor}$ indices of SAPs whilst the remaining indices are discarded. For example, SAPs of [1, 2], [2, 3], [3, 4] and [1, 4] are used in $n = 4$, $k = 2$ index combination whilst [1, 3] and [2, 4] are discarded to convey 2 index bits. To measure the SAPs utilization rate in a subblock, we introduce the parameter

$$\alpha = \frac{2^{\lfloor \log_2 C(n,k) \rfloor}}{C(n, k)} \quad (2)$$

This parameter shows the rate of the SAPs used to transmit index bits compared to all SAPs in each subblock. Considering ε subblocks, the number of SAPs used by OFDM-IM is $\left[2^{\lfloor \log_2 C(n,k) \rfloor} \right]^\varepsilon$, whilst the number of all possible SAPs in ε subblocks is $C^\varepsilon(n, k)$. Thus the SAPs utilization rate of ε subblocks can be presented by α^ε. It worth noted that when α is not close to 1, α^ε will dramatically decrease as the increase of ε. In other word, concentrating on the SAPs of each subblock, all indices of the SAPs have been fully extracted to transmit index bits, but those indices of discarded SAPs in each subblocks are accumulated when considering ε subblocks, which leads to a large waste in index domain especially in lower α.

After the inverse fast Fourier transform (IFFT) and cyclic prefix (CP) operation, the signal in time domain is output into a frequency-selective Rayleigh fading channel with the length of υ which can be presented by channel impulse coefficients
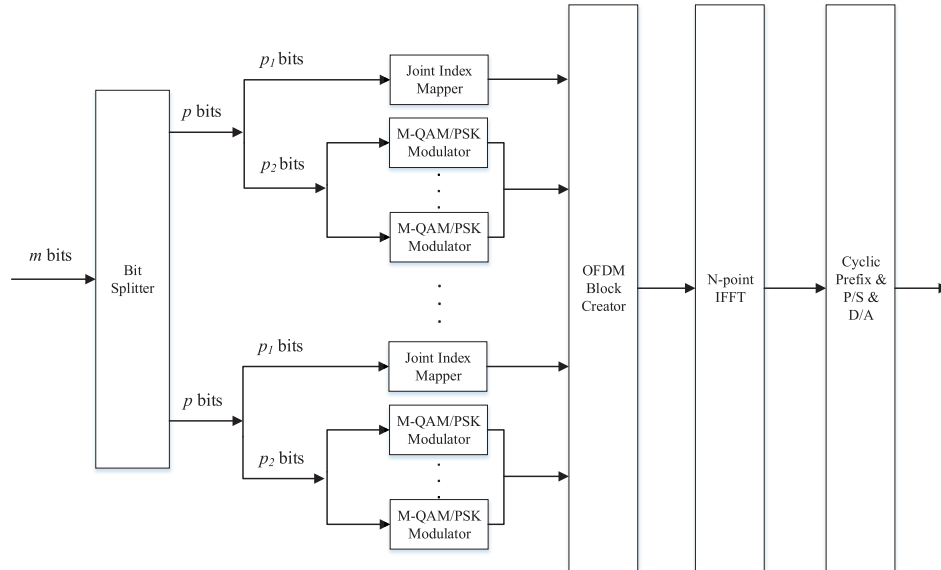
FIGURE 1. Block diagram of OFDM-JS-IM transmitter.

$h_T = [h_T(1), \ldots, h_T(\upsilon)]^T$ where $h_T(\sigma) \sim \mathcal{CN}(0, \frac{1}{\upsilon})$, $\sigma = 1, \ldots, \upsilon$ and the length of CP is assumed to be larger than υ. In the receiver, CP is removed and the FFT algorithm is applied, the received signal can be given by

$$y_F = Xh_F + w_F, \tag{3}$$

where X is an $N \times N$ diagonal matrix of which main diagonal element are given by $x(1), \ldots, x(N)$. $h_F = [h_F(1), \ldots, h_F(N)]^T = W_N h_T^0$ is the frequency channel vector where h_T^0 is the zero-padded version of h_T at the length of N and W_N is the N-point discrete Fourier transform (DFT). w_F is the noise vector in the frequency domain with the distribution $\mathcal{CN}(0, N_{0,F}I_N)$, where $N_{0,F}$ is the noise variance in the frequency domain. It should be noted that elements of h_F are no longer an uncorrelated after DFT operation. The correlation matrix of h_F is given by K, where $K = E\{h_F h_F^T\} = W_N^H \widetilde{I} W_N$ and $\widetilde{I}$ is the $N \times N$ zero matrix except its main diagonal element is a zero-padded version of the vector $[\frac{1}{\upsilon}, \frac{1}{\upsilon}, \ldots, \frac{1}{\upsilon}]_{1 \times \upsilon}$.

From the principle of OFDM-IM scheme, it is shown that the SAPs utilization rate α may be much lower than 1 due to the mismatch between the number of SAPs and binary bits in each subblock. As a result, the waste of SAPs are dramatically accumulated when considering ε subblocks. To reuse these discarded SAPs and increase the spectral efficiency, OFDM with joint subblocks index modulation are proposed as follows.

III. PRINCIPLE OF OFDM-JS-IM SCHEME
A. TRANSMITTER MODEL FOR OFDM-JS-IM
The block diagram of the OFDM-JS-IM transmitter is shown in Fig. 1. The transmitter divides m-bits information into g groups, where each group consisting of p-bits, so $p = m/g$. Each group of p-bits information is partitioned into p_1-bits fed

Algorithm 1 Mapping From the p_1-Bits to Joint Indices of SAPs
___
Step1: Calculate the incoming $p_1 = \lfloor \log_2(C^L(n, k)) \rfloor$ index bits for index mapper.
Step2: Convert incoming binary p_1-bits into the $C(n, k)$-based integer Z at the length of L. Then the joint index of SAPs can be presented by a set $\{Index\ 1, \ldots, Index\ L\}$.
Step3: For μth subblock in βth group, the relationship between indices of SAPs, I_β^μ and Index μ is given by Table 1. Hence, the indices of L joint subblocks $\{I_\beta^1, \ldots, I_\beta^L\}$ are calculated and then put into OFDM block creator.
___

into joint index mapper and p_2-bits for L modulators, where L is the length of joint subblocks contained in each group. It is worth noted that in OFDM-IM, an index mapper determined the indices of only one subblock and p_2-bits are fed into only one M-QAM/PSK modulator. Let us focus on μth subblock of βth group. Similarly in OFDM-IM, k subcarriers are selected as active ones out of n subcarriers. The indices of k subcarriers selected as active subcarriers are presented by I_β^μ, which is given by

$$I_\beta^\mu = \left\{ i_{\beta,1}^\mu, \ldots, i_{\beta,k}^\mu \right\}, \tag{4}$$

where $i_{\beta,\kappa}^\mu \in \{1, \ldots, n\}$ for $\mu = 1, \ldots, L$, $\beta = 1, \ldots, g$ and $i_{\beta,\kappa_1}^\mu \neq i_{\beta,\kappa_2}^\mu$. The remaining n-k subcarriers are set to be idle. In the proposed scheme, βth group combines the indices of all L subblocks through the joint index mapper which builds a mapping from p_1 binary bits to joint indices of L subblocks represented by $\{I_\beta^1, \ldots, I_\beta^L\}$. The algorithm used in the joint index mapper is presented as follows.

TABLE 1. The comparison between the index in OFDM-IM with $(n, k) = (4, 2)$ and joint indices in OFDM-JS-IM with $(n, k, L) = (4, 2, 2)$.

OFDM-IM		OFDM-JS-IM			
$Index$	I_β	$Index\,1$	$I_\beta^{\mu=1}$	$Index\,2$	$I_\beta^{\mu=2}$
0	$[1,2]$	0	$[1,2]$	0	$[1,2]$
1	$[2,3]$	1	$[2,3]$	1	$[2,3]$
2	$[3,4]$	2	$[3,4]$	2	$[3,4]$
3	$[1,4]$	3	$[1,4]$	3	$[1,4]$
4	discard	4	$[1,3]$	4	$[1,3]$
5	discard	5	$[2,4]$	5	$[2,4]$

In Table 1, index combination $(n, k) = (4, 2)$ used in OFDM-IM and the joint index combination $(n, k, L) = (4, 2, 2)$ used in OFDM-JS-IM are presented. In OFDM-IM scheme, two SAPs out of six are discarded to convey 2 index bits whilst in the joint index mapper of OFDM-JS-IM, 32 joint indices of SAPs presented by {*Index* 1, *Index* 2} from $\{0, 0\}$ to $\{5, 1\}$ out of 36 possible joint indices of SAPs from $\{0, 0\}$ to $\{5, 5\}$ are used to convey 5 index bits. For example, when incoming p_1-bits is '01101', it can be mapped to a 6-based integer $Z = 21$ namely {*Index* 1, *Index* 2} = $\{2, 1\}$. Therefore, the modulators use the SAPs mapping to *Index* $1 = 2$ and *Index* $2 = 1$ according to Table 1.

The second part, the comprised of p_2-bits selects kL symbols for M-ary complex signals. For each modulator, k symbols are mapped by normalized M-ary constellation point set, yielding

$$s_\beta^\mu = \left[s_{\beta,1}^\mu, \ldots, s_{\beta,k}^\mu \right]^T, \tag{5}$$

where $s_{\beta,\kappa}^\mu$ is the complex M-ary signal to be transmitted over the subcarrier of index $i_{\beta,\kappa}^\mu, \kappa = 1, \ldots, k$. After the operations of OFDM block creator, all OFDM symbols are converted into time domain through IFFT operation and the addition of cyclic prefix (CP). Then parallel to serial (P/S) and digital-to-analog conversion (DA) are applied before the signals are transmitted through Rayleigh fading channel. The SE of OFDM, OFDM-IM and OFDM-JS-IM can be derived as

$$\eta_{\text{OFDM}} = \frac{N \log_2 M}{N + L_{\text{CP}}} \tag{6}$$

$$\eta_{\text{OFDM-IM}} = \frac{N \left(\log_2 M^k + \lfloor \log_2(C(n, k)) \rfloor \right)}{n(N + L_{\text{CP}})} \tag{7}$$

$$\eta_{\text{OFDM-JS-IM}} = \frac{N \left(\log_2 M^k + \lfloor \log_2(C(n, k)^L) \rfloor / L \right)}{n(N + L_{\text{CP}})}, \tag{8}$$

where M is the M-ary symbol transmitted by p_2-bits and L_{CP} is the length of cyclic prefix. Let us focus on spectral efficiencies of OFDM-JS-IM and OFDM-IM. When L subblocks were jointed, the index bits are $p_1 = \lfloor \log_2(C^L(n, k)) \rfloor$ bits whilst in OFDM-IM the index bits of each subblock are $p_1 = \lfloor \log_2(C(n, k)) \rfloor$ bits. Therefore, the relationship about index bits of L subblocks between two schemes can be easily given by

$$\lfloor \log_2(C^L(n, k)) \rfloor \geqslant L \times \lfloor \log_2(C(n, k)) \rfloor \tag{9}$$

From (7), (8) and (9)

$$\eta_{\text{OFDM-JS-IM}} \geqslant \eta_{\text{OFDM-IM}}, \tag{10}$$

which proves that OFDM-JS-IM is available to increase the SE of OFDM-IM. Assuming $N = 128$, $L_{\text{CP}} = 16$ and $(n, k, L) = (4, 2, 2)$ with employment of BPSK, η_{OFDM}, $\eta_{\text{OFDM-IM}}$, $\eta_{\text{OFDM-JS-IM}}$ are calculated to be 0.8889 bit/s/Hz, 0.8889 bit/s/Hz and 1bits/s/Hz, where 0.1111 bits/s/Hz spectral efficiency is attained through the proposed OFDM-JS-IM scheme over OFDM-IM and OFDM scheme. Concentrating on index bits conveyed by SAPs indices, 25% improvement of additional index bits is gained in (4, 2, 2) OFDM-JS-IM. Note that the proposed OFDM-JS-IM scheme increases the SE without extra consumption, only by reusing the discarded SAPs. Hence, OFDM-JS-IM scheme also improves the energy efficiency compared to original OFDM-IM scheme.

B. SELECTION OF PROPER LENGTH OF JOINT SUBBLOCKS
In this subsection, the selection of the proper value of L is discussed to convey more extra index bits. As the increase of L, more subblocks are combined to produce joint index, which may enhance the spectral efficiency. However, if unused joint SAPs have not been accumulated enough to convey extra bits or only a few extra bits through a vast number of joint subblocks, it is not necessary to use these values of L as the length of joint subblocks. To clearly explain the function of joint index mapper to fully use the SAPs, the following inequation is given by

$$\alpha^L \cdot 2^{\Delta p_1} \leqslant 1, \tag{11}$$

where α^L is regarded as the SAPs utilization rate of L joint subblocks and Δp_1 represents the additional incoming index bits conveyed with L joint subblocks. It is worth noted that for one-unit increase of Δp_1, the joint indices used are double the indices of the previous one. Thus the number of joint indices of SAPs in OFDM-JS-IM is $2^{\Delta p_1}$ times the number of indices SAPs in OFDM-IM. Since we cannot completely use up all the indices of SAPs in most of cases, the left part of the inequation is smaller than 1. According to (11), the method of calculating the minimum joint length can be given by

$$L_{min} = \left\lceil \log_\alpha \left(\frac{1}{2^{\Delta p_1}} \right) \right\rceil \tag{12}$$

From (12), the value of L_{min} can be calculated when Δp_1, n and k are determined. Hence, the selection of L can be limited to the set of L_{min}. In addition, we notice that the relationships between some L_{min} and their corresponding Δp_1 are linear, namely the some of L_{min} cannot transmit extra index bits. For example, when (n, k)=(4, 2), we calculate that $L_{min} = 2, 4$ and 6 corresponding to $\Delta p_1 = 1, 2$ and 3 bits, and therefore the $L_{min} = 4$ and $L_{min} = 6$ are not the proper length since no extra bits are conveyed compared to $L_{min} = 2$ at the same length of subcarriers. To further select the proper L_{min}, we introduce the parameter

$$\varphi = \frac{\Delta p_1}{n \cdot L_{min}} \tag{13}$$

TABLE 2. The proper length of joint subblocks $L_{\min}$ (underlined), SAPs utilization rate α and φ in common index combinations (n, k).

(n, k)	α	Δp_1								
		0bits		1bits		2bits		3bits		4bits	
		L	φ	$L_{\min}$	φ	$L_{\min}$	φ	$L_{\min}$	φ	$L_{\min}$	φ
$(4, 2)$	2/3	1	0	2	0.125	4	0.125	6	0.125	7	0.143
$(6, 3)$	4/5	1	0	4	0.042	7	0.048	10	0.050	13	0.0513
$(8, 6)$	4/7	1	0	2	0.063	3	0.083	4	0.094	5	0.100
$(8, 3)$	4/7	1	0	2	0.063	3	0.083	4	0.094	5	0.100
$(8, 4)$	32/35	1	0	8	0.016	16	0.016	24	0.016	31	0.0161

The ratio φ calculates the extra bits can be transmitted per subcarrier. For the transmitter, the L_{min} with the larger φ (underlined in Table 2) can be selected as the potential length of joint subblocks. The value of α and φ in the common index combination (n, k) are listed in Table 2. It is shown that $(8, 6)$, $(8, 3)$ and $(4, 2)$ have a lower α than others, which means that more discarded indices can be reused to enhance SE. In addition, those index combinations with $\alpha \approx 1$ such as $(8, 4)$ are not suitable for the proposed scheme since only a few bits can be transmitted with a large value of L_{min}, which will introduce a large error propagation.

IV. DETECTION FOR OFDM-JS-IM SCHEME

In OFDM-JS-IM scheme, we reuse most of discarded SAPs to convey more index bits. However, the structure of system is changed by joint subblocks, which involves more searching steps of the detection since the search units are expanded to joint subblocks. Considering the utilization of the ML detector, all possible joint indices and M-ary constellation signals are detected by the group of L joint subblocks. The computational complexity of the ML detector is $\sim \mathcal{O}(2^{\log_2^L C(n,k)} M^{Lk})$, which is quite unpractical for implementation.

In this section, we discuss two reduced-complexity detectors for OFDM-JS-IM. Before that, the block diagram of the receiver is given in Fig. 2. The received OFDM symbols are partitioned into g groups and each group contains L joint subblocks. For each subblock, the detector is used to calculate the indices and constellation signals. Then the indices of each group are put into the joint index demapper which contains reverse steps of Algorithm 1 introduced in Section II whilst the constellation signals are fed into the M-ary constellation demapper.

A. NEAR MAX LIKELIHOOD (ML) DETECTOR

Similar to ML detector, near-ML detector considers all possible SAPs and signal constellation points of each active subcarrier, which calculates the minimum Euclidean distance. It is worth noted that near-ML detector detects the indices of SAPs by each subblock rather than by the group of joint subblocks in the ML detector. Hence, indices of SAPs and constellation signals of each subblock I_β^μ can be calculated via

$$(\widehat{I}_\beta^\mu, \widehat{s}_\beta^\mu)$$

$$= \arg \min_{I_\beta, s_\beta} \sum_{\kappa=1}^{k} \left| y_{F,\beta}^\mu(i_{\beta,\kappa}^\mu) - h_{F,\beta}^\mu(i_{\beta,\kappa}^\mu) s_{\beta,\kappa}^\mu \right|^2 h_{F,\beta}^\mu(\xi) \quad (14)$$

where $y_{F,\beta}^\mu(\xi)$ and $h_{F,\beta}^\mu(\xi)$ for $\xi = 1, \ldots, n$ are the received signals and the corresponding channel fading coefficients of βth group and μth subblock. It can be presented that $y_{F,\beta}^\mu(\xi) = y_F(\frac{N}{g}(\beta - 1) + (\mu - 1)n + \xi)$ and $h_{F,\beta}^\mu(\xi) = h_F(\frac{N}{g}(\beta - 1) + (\mu - 1)n + \xi)$.

The computational complexity of near-ML detector is $\sim \mathcal{O}(2^{\log_2(C(n,k))} M^k)$, which is much lower than ML detector. This detector is classified as near-ML since the receiver does not know all the legitimate joint indices. In other words, the receiver regards all of the joint indices as available through a small subset of joint indices are discarded. However, the computational complexity of near-ML detector increases highly like ML detector in OFDM-IM with the increase of n and k, which may be unpractical for implementation. To decrease the complexity of the demapping, the other reduced complexity detection for OFDM-JS-IM was proposed as follows.

B. LOG-LIKELIHOOD RATIO (LLR) DETECTOR

The logarithm of the ratio of a posteriori probabilities of each subcarrier for the original LLR detector can be calculated to detect the idle subcarrier or active subcarrier. Similarly, the ratio is formulated as [11]

$$\lambda(r) = \ln(k) - \ln(n - k) + \frac{|y_F(r)|^2}{N_{0,F}}$$
$$+ \ln \left(\sum_{m=1}^{M} \exp \left(-\frac{1}{N_{0,F}} |Y(r) - H(r) s_m|^2 \right) \right),$$
(15)

where $r = 1, \ldots, N$, $s_m \in S$ and S is the set of M-ary constellation symbols. In each subblock of OFDM-JS-IM, k highest probabilities out of n are assumed to be active, which can be presented by

$$d_{\beta,\omega}^\mu = \sum_{\kappa=1}^{k} \lambda(\frac{N}{g}(\beta - 1) + (\mu - 1)n + i_{\beta,\kappa}^\mu), \quad (16)$$

where $\omega = 1, \ldots, C(n, k)$. Considering Table I, assuming that $\beta = 1$ and $\mu = 1$, we get that $d_{\beta,1}^\mu = \lambda(1) + \lambda(2)$, $d_{\beta,2}^\mu = \lambda(2) + \lambda(3)$, $d_{\beta,3}^\mu = \lambda(3) + \lambda(4)$, $d_{\beta,4}^\mu = \lambda(1) + \lambda(4)$, $d_{\beta,5}^\mu = \lambda(1) + \lambda(3)$ and $d_{\beta,6}^\mu = \lambda(2) + \lambda(4)$. Compared to OFDM-IM, $d_{\beta,5}^\mu$ and $d_{\beta,6}^\mu$ are the extra computational cost. However, the calculations of LLR sums are very simple for LLR detection and therefore the order of computational complexity of OFDM-JS-IM is the same as that of OFDM-IM,
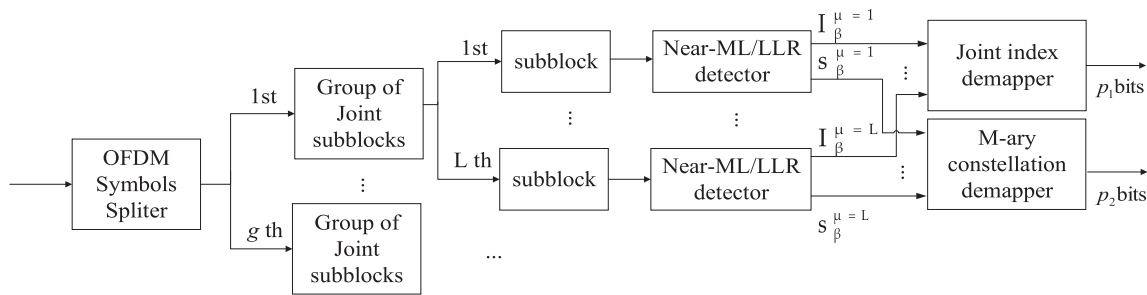
FIGURE 2. Block diagram of the OFDM-JS-IM receiver.

which is $\sim \mathcal{O}(M)$ per subcarrier. After calculating all $C(n,k)$ LLR sums for each subblock, the I_β^μ can be decided by the max LLR sums in the receiver and the demodulation of the M-ary constellation symbols is straightforward for the receiver.

TABLE 3. Complexity comparison between ML, near ML and LLR detectors.

(n, k, L)	ML	Near-ML	LLR
$(4, 2, 2)$	512	144	2
$(8, 3, 2)$	131072	448	2
$(8, 6, 2)$	2097152	1792	2

Consequently, the computational complexity of ML, near-ML and LLR detectors can be presented by $2^{\log_2^L C(n,k)} M^{Lk}$, $2^{\log_2(C(n,k))} M^k$ and M. As seen from Table 3, the comparison results of different (n, k, L) with employment of BPSK ($M = 2$) represents that the reduced complexity LLR detector has the lowest computational complexity whilst the ML detector suffers from extremely high computational complexity.

V. PERFORMANCE ANALYSIS OF OFDM-JS-IM

The average PEP (APEP) calculation can be utilized to acquire the asymptotically tight upper bound for the performance of OFDM-JS-IM. During the analysis, each group containing L joint subblocks are required to be considered, for the reason that the PEP events in different group are mutually independent. By considering the first group of L joint subblocks, the conditional PEP (CPEP) of the event can be presented by

$$\Pr\left(X^{(1,...,L)} \to \hat{X}^{(1,...,L)} | H_{(1,...,L)}\right) = Q\left(\sqrt{\frac{\rho}{2N_{0,F}}}\right), \quad (17)$$

where $X^{(1,...,L)}$ is an $nL \times nL$ all zero matrix except for its diagonal elements are the symbols of L joint subblocks and $X^{(1,...,L)}$ is mistakenly detected as $\hat{X}^{(1,...,L)}$.

$$\rho = \left\| \text{diag}\left\{ X^{(1,...,L)} - \hat{X}^{(1,...,L)} \right\} H_{(1,...,L)} \right\|_2^2 \quad (18)$$

Then the unconditional PEP (UPEP) can be presented by

$$\Pr\left(X^{(1,...,L)} - \hat{X}^{(1,...,L)}\right) = E_{H_{(1,...,L)}}\left\{ Q\left(\sqrt{\frac{\rho}{2N_{0,F}}}\right)\right\}, \quad (19)$$

where $E_{H_{(1,...,L)}}\{\cdot\}$ is the expectation with respect to the channel coefficients $H_{(1,...,L)}$ and $Q(\cdot)$ is the Gaussian Q-function.

To simplify the expression of Q-function, exponential sums (Prony approximation) [23] can be applied to present the upper bound as

$$Q(x) \approx \frac{1}{12}e^{-x^2/2} + \frac{1}{4}e^{-2x^2/3} \quad (20)$$

Moreover, we use the more approximative expression provided in [24] for Q-function in order to achieve the tighter upper BER bound as

$$Q(x) \approx 0.168e^{-0.876x^2} + 0.144e^{-0.525x^2} + 0.002e^{-0.603x^2} \quad (21)$$

which has been adopt in [15]. Using the spectral theorem [25], (19) and (21) can be briefly derived as [11]

$$\Pr\left(X^{(1,...,L)} - \hat{X}^{(1,...,L)}\right)$$

$$\approx \frac{1}{1/0.168 \det\left(\mathbf{I}_{nL} + \frac{0.876}{2N_{0,F}}\mathbf{K}_{nL}\mathbf{A}\right)}$$

$$+ \frac{1}{1/0.144 \det\left(\mathbf{I}_{nL} + \frac{0.525}{2N_{0,F}}\mathbf{K}_{nL}\mathbf{A}\right)}$$

$$+ \frac{1}{1/0.002 \det\left(\mathbf{I}_{nL} + \frac{0.603}{2N_{0,F}}\mathbf{K}_{nL}\mathbf{A}\right)}, \quad (22)$$

where $\mathbf{I}_{nL}$ denotes the $nL \times nL$ identity matrix, $\mathbf{K}_{nL} = E\left\{H_{(1,...,L)}H_{(1,...,L)}^H\right\}$, which can be simplified as the $nL \times nL$ submatrix centered along the main diagonal of the matrix K and $\mathbf{A} = \left(X^{(1,...,L)} - \hat{X}^{(1,...,L)}\right)^H \left(X^{(1,...,L)} - \hat{X}^{(1,...,L)}\right)$. After considering all of conditions of UPEP events, the APEP can be presented as

$$\Pr_{avg} \approx \frac{1}{pn_{X^{(1,...,X)}}} \sum_{X^{(1,...,L)}} \sum_{\hat{X}^{(1,...,L)}}$$

$$P\left(X^{(1,...,L)} \to \hat{X}^{(1,...,L)}\right) e\left(X^{(1,...,L)}, \hat{X}^{(1,...,L)}\right), \quad (23)$$

where $n_{X^{(1,...,L)}}$ is the number of the possible realizations of $X^{(1,...,L)}$ and $e\left(X^{(1,...,L)}, \hat{X}^{(1,...,L)}\right)$ represents the number of bit errors for the corresponding pairwise error event.

It worth notes that the approximation of the Gaussian Q-function works well when the value of x is within the fittest region of $Q(x)$. On the contrary, when x is beyond the fittest region ($x < 0.5$), which means that high order constellation is employed or under the low SNR conditions, much more CPEP results suffer the deviations compared to simulated BER. Therefore, theoretical APEP introduces more inevitable estimation errors due to the deviations of CPEP especially in low SNR region.

VI. RESULTS AND DISCUSSION

In this section, simulations are carried out to evaluate the BER performance of OFDM-JS-IM under AWGN and Rayleigh fading channel. Assume that the length of CP is $L_{CP} = 16$ and the length of Rayleigh channel fading coefficients is $\upsilon = 10$ with the employment of BPSK modulation.
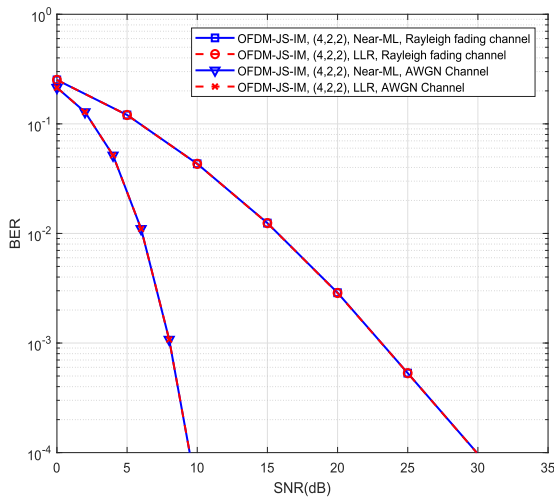
FIGURE 3. BER performance of OFDM-JS-IM used near-ML detector and LLR detector in Rayleigh fading channel and AWGN channel, *N* = 128.

As seen from Fig. 3, the BER performances of near-ML detector and LLR detector are very close (almost coincide), which can be explained by the fact that both of detectors ignore the unused joint SAPs. Thus the LLR detector is better than near-ML detector in the proposed scheme due to the lower computational complexity. To clearly present the results, the results based by near-ML detector are removed in the following curves.

The BER performance comparison between classical OFDM and OFDM-JS-IM (4, 2, 2) based on LLR detector under Rayleigh fading channel and AWGN channel is illustrated at Fig. 4. The spectral efficiencies of classical OFDM and OFDM-JS-IM (4, 2, 2) are 0.8889 bits/s/Hz and 1 bits/s/Hz. It is shown that the proposed scheme achieves about 5 dB performance improvement at high SNR region under Rayleigh fading channel and suffers slight performance loss under AWGN channel with 0.1111 bits/s/Hz improvement of SE. At low SNR, the BER performance of OFDM-JS-IM (4, 2, 2) under Rayleigh fading channel suffers performance loss. However, the advantage of IM technique
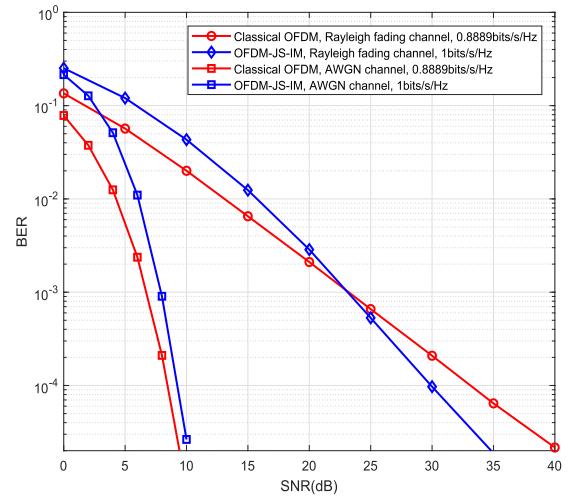

FIGURE 4. BER performance of classical OFDM and OFDM-JS-IM in Rayleigh fading channel and AWGN channel, *N* = 128.

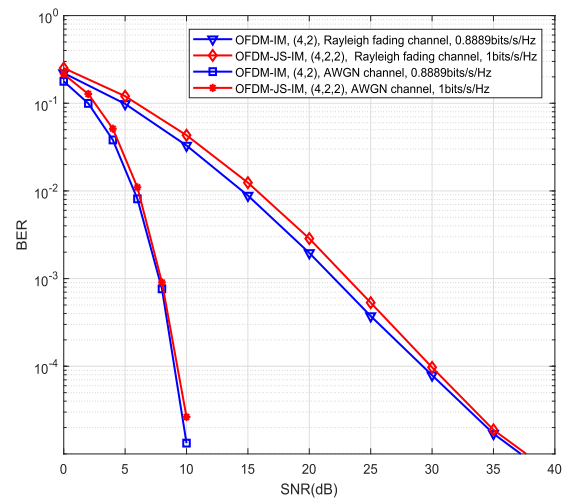presents at high SNR and therefore the loss of performance at low SNR region is negligible.

FIGURE 5. BER performance of OFDM-IM (4, 2) and OFDM-JS-IM (4, 2, 2) in Rayleigh fading channel and AWGN channel, *N* = 128.

Fig. 5 illustrates the BER performances of OFDM-IM (4, 2) and OFDM-JS-IM (4, 2, 2) under the Rayleigh fading channel and AWGN channel. The spectral efficiencies of OFDM-IM (4, 2) and OFDM-JS-IM (4, 2, 2) are 0.8889 bits/s/Hz and 1 bits/s/Hz, which has the 0.1111 bits/s/Hz improvement of SE. At low SNR region, the proposed scheme suffers from only 1dB BER performance loss than OFDM-IM, this can be understood that joint index mapper introduces the error propagation of the indices. In medium and high SNR region, the performance of OFDM-JS-IM is gradually close to that of OFDM-IM because the constellation signals errors are the major impact of BER performance at this region. Besides, the BER performance between OFDM-IM and OFDM-JS-IM is very close under AWGN channel.
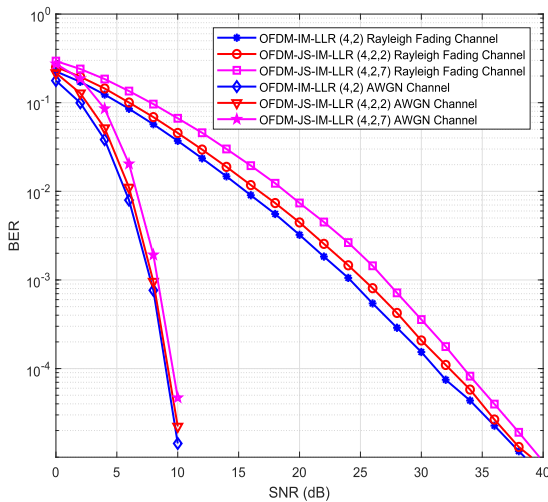
FIGURE 6. BER performance of OFDM-IM (4, 2), OFDM-JS-IM (4, 2, 2) and OFDM-JS-IM (4, 2, 7) in Rayleigh fading channel and AWGN channel, $N = 280$.

FIGURE 7. BER performance of OFDM-IM (4, 2) and OFDM-JS-IM (4, 2, 2) with employment of BPSK, QPSK and 16QAM in Rayleigh fading channel, $N = 128$.

FIGURE 8. Comparison between the theoretical APEP analysis and the simulated BER performance of the proposed OFDM-JS-IM with the employments of BPSK and QPSK in Rayleigh fading channel.

In Fig. 6, the BER performance of OFDM-IM, OFDM-JS-IM (4, 2, 4) and OFDM-JS-IM (4, 2, 7) are illustrated. To partition the subcarriers into groups at $L = 4$ and $L = 7$, the number of subcarriers is set as $N = 280$. The spectral efficiencies of OFDM-IM, OFDM-JS-IM (4, 2, 4) and OFDM-JS-IM (4, 2, 7) are 0.945 bits/s/Hz, 1.06 bits/s/Hz and 1.08 bits/s/Hz. It can be seen that aside from the 0.135 bits/s/Hz enhancement of SE, OFDM-JS-IM with $L = 7$ suffers about 1dB performance loss at high SNR region compared to OFDM-IM. Thus, there exists a trade-off between the SE and BER performance by the selection of L of different (n, k). Besides, it is shown that performance deviation of OFDM-JS-IM (4, 2, 7) and OFDM-JS-IM (4, 2, 2) gradually decreases at high SNR. It can be demonstrated that errors mainly stem from the ordinary modulation bits at this region even if the errors of index bits are propagated at $L = 7$ joint subblocks.

Fig. 7 depicts the comparisons between OFDM-IM (4, 2) and OFDM-JS-IM (4, 2, 2) with the employments of BPSK, QPSK and 16QAM. The SEs of OFDM-IM (4, 2) with BPSK, QPSK and 16QAM are 0.8889bits/s/Hz, 1.3333bits/s/Hz and 2.2222bits/s/Hz, whilst for OFDM-JS-IM (4, 2, 2) the SEs are 1bits/s/Hz, 1.4444bits/s/Hz and 2.3333bits/s/Hz, among which the 0.1111bits/s/Hz enhancement are achieved by OFDM-JS-IM. It can be observed that the BER performance loss of OFDM-JS-IM compared to classical OFDM-IM obviously decreases (nearly negligible) as the increase of modulation order. It can be explained that higher modulation order introduces the smaller average Euclid distance, which causes much more errors of ordinary modulation bits. Meanwhile, the proportion of ordinary modulation bits is increased in higher order modulation and therefore the error propagation caused by false detection of joint index bits is diluted. In other words, most of errors stems from the ordinary modulation bits in this case. As a result, OFDM-JS-IM scheme is significant to enhance the spectral efficiency of classical OFDM-IM scheme, especially in higher order modulation cases.
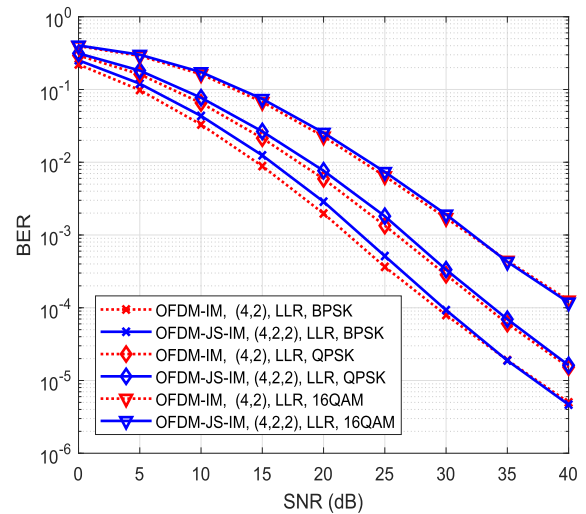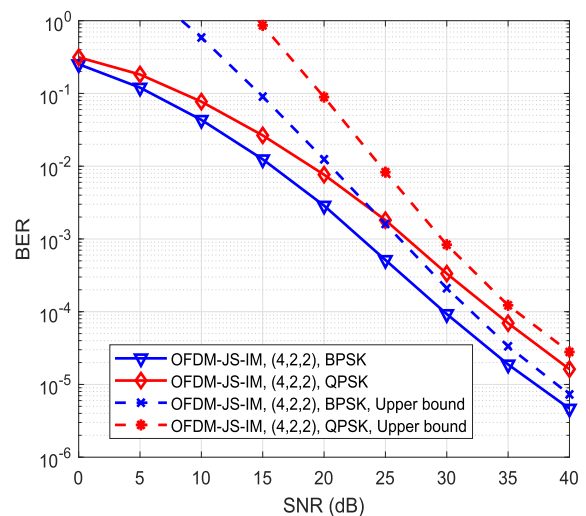
Moreover, in Fig. 8, the comparison between the simulated BER performance results of OFDM-JS-IM (4, 2, 2) with the employments of BPSK and QPSK and its corresponding APEP theoretical results is depicted under the Rayleigh fading channel. Based on the union bound, the APEP theoretical results can be regarded as the upper bound of the computer simulation. It shows that inevitable difference exists at low SNR region, which can be explained by the more PEP events introduced by joint subblocks operation compared to that of OFDM-IM. As a result, more approximative errors of PEP due to the unbefitting approximation of Q-function at low SNR region are accumulated. However, as the rise of SNR, the deviation decreases gradually and the APEP theoretical results fit well with the simulated BER performance, which demonstrates the correctness of theoretical analysis.

VII. CONCLUSION

In this paper, OFDM-JS-IM is proposed to improve the spectral efficiency and energy efficiency of OFDM-IM without enhancing the system complex of transmitter and receiver. In the proposed scheme, a subset of subblocks are combined to produced joint indices, through which extra index bits can be conveyed. Besides, the selection of proper length of joint subblocks suitable for common index combinations is discussed to fully use SAPs. Moreover, the low-complexity near-ML detector and LLR detector are proposed for demodulation. The result shows that reduced complexity LLR detector performs well at both computation complexity and BER performance. In addition, there exists a trade-off between BER performance and spectral efficiency by the selection of length of joint subblocks. For higher order modulation of OFDM-JS-IM scheme, the performance loss become slighter, which indicates that OFDM-JS-IM scheme outperforms compared to OFDM-IM especially in higher spectral efficiency systems.

REFERENCES

[1] R. van Nee and R. Prasad, *OFDM for Wireless Multimedia Communications*. 2000.

[2] D. Astely, E. Dahlman, A. Furuskär, Y. Jading, M. Lindström, and S. Parkvall, "LTE: The evolution of mobile broadband," *IEEE Commun. Mag.*, vol. 47, no. 4, pp. 44–51, Apr. 2009.

[3] A. Ghosh, R. Ratasuk, B. Mondal, N. Mangalvedhe, and T. Thomas, "LTE-advanced: Next-generation wireless broadband technology [invited paper]," *IEEE Wireless Commun.*, vol. 17, no. 3, pp. 10–22, Jun. 2010.

[4] G. L. Stüber, J. R. Barry, S. W. McLaughlin, Y. Li, M. A. Ingram, and T. G. Pratt, "Broadband MIMO-OFDM wireless communications," *Proc. IEEE*, vol. 92, no. 2, pp. 271–294, Feb. 2004.

[5] R. Y. Mesleh, H. Haas, S. Sinanovic, C. W. Ahn, and S. Yun, "Spatial modulation," *IEEE Trans. Veh. Technol.*, vol. 57, no. 4, pp. 2228–2241, Jul. 2008.

[6] E. Basar, M. Wen, R. Mesleh, M. Di Renzo, Y. Xiao, and H. Haas, "Index modulation techniques for next-generation wireless networks," *IEEE Access*, vol. 5, pp. 16693–16746, 2017.

[7] E. Başar, "Index modulation techniques for 5G wireless networks," *IEEE Commun. Mag.*, vol. 54, no. 7, pp. 168–175, Jul. 2016.

[8] T. Mao, Q. Wang, Z. Wang, and S. Chen, "Novel index modulation techniques: A survey," *IEEE Commun. Surveys Tuts.*, to be published.

[9] R. Abu-Alhiga and H. Haas, "Subcarrier-index modulation OFDM," in *Proc. IEEE Int. Symp. Pers.*, Sep. 2009, pp. 177–181.

[10] D. Tsonev, S. Sinanovic, and H. Haas, "Enhanced subcarrier index modulation (SIM) OFDM," in *Proc. IEEE Global Commun. Conf. Workshops (GLOBECOM Wkshps)*, Dec. 2011, pp. 728–732.

[11] E. Başar, U. Aygölü, E. Panayırcı, and H. V. Poor, "Orthogonal frequency division multiplexing with index modulation," *IEEE Trans. Signal Process.*, vol. 61, no. 22, pp. 5536–5549, Nov. 2013.

[12] R. Fan, Y. J. Yu, and Y. L. Guan, "Generalization of orthogonal frequency division multiplexing with index modulation," *IEEE Trans. Wireless Commun.*, vol. 14, no. 10, pp. 5350–5359, Oct. 2015.

[13] T. Mao, Z. Wang, Q. Wang, S. Chen, and L. Hanzo, "Dual-mode index modulation aided OFDM," *IEEE Access*, vol. 5, pp. 50–60, Feb. 2017.

[14] T. Mao, Q. Wang, and Z. Wang, "Generalized dual-mode index modulation aided OFDM," *IEEE Commun. Lett.*, vol. 21, no. 4, pp. 761–764, Apr. 2017.

[15] T. Mao, Q. Wang, J. Quan, and Z. Wang, "Zero-padded orthogonal frequency division multiplexing with index modulation using multiple constellation alphabets," *IEEE Access*, vol. 5, pp. 21168–21178, 2017.

[16] M. Wen, E. Basar, Q. Li, B. Zheng, and M. Zhang, "Multiple-mode orthogonal frequency division multiplexing with index modulation," *IEEE Trans. Commun.*, vol. 65, no. 9, pp. 3892–3906, Sep. 2017.

[17] M. Wen, B. Ye, E. Basar, Q. Li, and F. Ji, "Enhanced orthogonal frequency division multiplexing with index modulation," *IEEE Trans. Wireless Commun.*, vol. 16, no. 7, pp. 4786–4801, Jul. 2017.

[18] M. I. Kadir, H. Zhang, S. Chen, and L. Hanzo, "Entropy coding aided adaptive subcarrier-index modulated OFDM," *IEEE Access*, vol. 6, pp. 7739–7752, 2018.

[19] S. Dang, G. Chen, and J. P. Coon, "Lexicographic codebook design for OFDM with index modulation," *IEEE Trans. Wireless Commun.*, vol. 17, no. 12, pp. 8373–8387, Dec. 2018.

[20] S. Dang, J. P. Coon, and G. Chen, "Adaptive OFDM with index modulation for two-hop relay-assisted networks," *IEEE Trans. Wireless Commun.*, vol. 17, no. 3, pp. 1923–1936, Mar. 2018.

[21] E. Başar, "OFDM with index modulation using coordinate interleaving," *IEEE Wireless Commun. Lett.*, vol. 4, no. 4, pp. 381–384, Aug. 2015.

[22] Q. Li, M. Wen, E. Basar, H. V. Poor, B. Zheng, and F. Chen, "Diversity enhancing multiple-mode OFDM with index modulation," *IEEE Trans. Commun.*, vol. 66, no. 8, pp. 3653–3666, Aug. 2018.

[23] M. Chiani and D. Dardari, "Improved exponential bounds and approximation for the Q-function with application to average error probability computation," in *Proc. IEEE Global Telecommun. Conf.*, Nov. 2002, pp. 1399–1402.

[24] P. Loskot and N. C. Beaulieu, "Prony and polynomial approximations for evaluation of the average probability of error over slow-fading channels," *IEEE Trans. Veh. Technol.*, vol. 58, no. 3, pp. 1269–1280, Mar. 2009.

[25] R. A. Horn and C. R. Johnson, *Matrix Analysis*. Cambridge, U.K.: Cambridge Univ. Press, 1985.

YUXIN SHI received the B.Sc. degree in communication engineering from the National University of Defense Technology, Changsha, Hunan, China, in 2016, where he is currently pursuing the M.Sc. degree with the Department of Communication Engineering, School of Electronic Science. His research interests include index modulation, wireless transmission, and physical layer security.

KAI GAO received the B.S., M.S., and Ph.D. degrees in electrical engineering from the National University of Defense Technology, Changsha, Hunan, China, in 2000, 2002, and 2006, respectively, where he was a Lecturer in information and communication engineering, from 2006 to 2009, and has been an Associate Professor in communication engineering, since 2009. He was an Academic Visitor with the University of Strathclyde, U.K., from 2016 to 2017. His current research interests include anti-interference communication, broadband wireless transmission, and communication countermeasures.

JIANG ZHU received the B.S., M.S., and Ph.D. degrees in electrical engineering from the National University of Defense Technology (NUDT), Changsha, Hunan, China, in 1994, 1997, and 2000, respectively, where he was a Lecturer in communication engineering, from 2000 to 2004. He was a Visiting Scholar with the University of Calgary, Calgary, AB, Canada, from 2004 to 2005. From 2005 to 2008, he was an Associate Professor in communication engineering with NUDT, where he has been a Full Professor with the School of Electronic Science and Engineering, since 2008. His current research interests include wireless high speed communication technology, satellite communication, physical layer security, and wireless sensor networks.

XINJIN LU received the B.Sc. degree in communication engineering from Hunan University, Changsha, China, in 2016, where she is currently pursuing the M.Sc. degree with the Department of Communication Engineering, School of Electronic Science. Her research interests include channel coding and physical layer security.

SHILIAN WANG received the B.S. and Ph.D. degrees in information and communication engineering from the National University of Defense Technology (NUDT), China, in 1998 and 2004, respectively.

Since 2004, he continued research in wireless communications with NUDT, where he later became a Professor, and is currently the Head of the Laboratory of Advanced Communication Technology, School of Electronic Science. From 2008 to 2009, he was a Visiting Scholar with the Department of Electronic and Electrical Engineering, Columbia University, New York City, NY, USA. He has authored or co-authored two books, 26 journal papers, and 20 conference papers. His research interests include wireless communications and signal processing theory, including chaotic spread spectrum and LPI communications, CPM and STC, underwater acoustic communication and networks, and deep learning and its applications in communication sensing.

● ● ●